Using the ESA MASTER-8 Model to Evaluate the State of Space Debris within the Medium-Earth Orbit Space Environment

Word Count: 4358

Context

Space has witnessed a surge of activity recently. With the recent success of commercial companies globally in providing cost-effective launch platforms based on new technologies, satellites and other orbital installations are now more feasible than ever before. These developments have led to more activity and focus in Earth's orbital space environment. However, this space activity does come with drawbacks, most importantly, the generation of space debris as a result.

Space debris is defined as derelict man-made objects mainly in Earth's orbit which no longer serve a function. These objects include propellants, mission-related debris, broken parts, abandoned launch stages, and non-functional satellites (Mehrholz Et Al., 2002). Space debris in orbit revolves around Earth at incredible speeds, containing an immense amount of kinetic energy despite being, on average, only centimeters wide. As a result, space debris is viewed negatively due to the fact that if it collides with other objects in orbit it will most certainly damage them to a great extent, even to the point of irreparability (Liou & Johnson, 2006).

The discussion of space debris and its impacts mostly center around its presence in Low-Earth Orbit (LEO), ranging from an orbital height of 160km to 2000km above Earth's surface. LEO, coupled with Medium-Earth Orbit (MEO) (2000km-35786km), and Geosynchronous Orbit (GEO) (35786km), form the three main Earth Centric Orbits as defined by the National Aeronautics and Space Administration (NASA) (Johnson, 2010). Space debris' long term effects escalate with an increase in orbit height, with debris in LEO remaining present for several years until it is sufficiently acted upon by atmospheric drag and pressure to fall back to earth, to debris in MEO and GEO, which will remain for several decades, even centuries, unless manually deorbited (Johnson, 2010).

Space debris is a significant problem and one that could get exponentially worse if left unchecked. Current research into space debris present at LEO, as is the scope of most space activity, has shown that the amount of debris is increasing at an exponential rate (Maury, 2019) . This has led to the discussion regarding space debris to largely center around LEO, with much research only considering the LEO space environment and its effects within that spectrum. However, with this focus, research surrounding other areas within the field of space debris has been neglected. Most significantly, the analysis of space debris and its effect on the Earth-Centric Orbits of Medium-Earth Orbit and Geosynchronous Orbit. In these spectrums, the variables considered when conducting analysis differ to a great extent, and to consider the full range of space debris, these areas must be analyzed separately. Of the two higher orbital spectrums, Medium-Earth Orbit is especially intriguing due to its middle-of-the-road nature. While satellites in Low-Earth Orbit can manually deorbit and burn up in the atmosphere (Smith Et At, 2020), and Geosynchronous satellites are able to be pushed into a graveyard orbit higher above Earth, where they will remain but will not be able to interfere with space operations (Colombo & Gkolias, 2017), Medium-Earth orbit is both too high and too low for these actions respectively. So this leaves satellites within this spectrum to remain as dangerous and potentially destructive space debris. Therefore, it is especially relevant to analyze the effects of space debris within MEO and their presence in the space environment to effectively characterize the full spectrum of space debris. As such, this paper seeks to understand to what extent Medium-Earth Orbital fragmentation events and resultant space debris has affected the corresponding space environment.

Literature Review

Due to the multi-aspect nature of the space debris issue, research in this particular field varies greatly in scope and scale. As of present, the existing body of research greatly focuses on space debris and its effects solely within the LEO spectrum. This is understandable as most human activity in space is confined to this area, with over 80% of all satellites being placed into this orbit. LEO has many advantages that are not present in other spectrums. LEO's proximity to earth results in less Delta-V[1] required for satellite placement in LEO, low latency for high-speed communication, and protection from outer space radiation allowing for less radiation-hardened components (Del Portillo Et Al, 2019). These benefits indicate why LEO has been chosen as the environment for a significant amount of space-based activity. However, while most space activity does occur in this spectrum, it is not the only area. Medium-Earth Orbit does host a sizable portion of satellite activity and therefore deserves the same level of research scrutiny as its lower-altitude counterpart.

Medium Earth Orbit (MEO) is the largest earth-centric orbit in terms of volume, ranging from 2000km to 35768km, containing around 12.5% of satellites (Maury, 2019). While this is significantly smaller than LEO in terms of sheer numbers, MEO hosts more mission-critical space systems, as MEO is the home of all global positioning system arrays. This includes the United States, Russia, China, India, and the European Union (Johnson, 2010), and as such when considering the possible effects of space debris within this spectrum MEO must be analyzed due to the nature of satellites within its orbit.

---

[1] Measure of the Impulse per Unit of Spacecraft Mass Needed to Perform a Maneuver

While there is a breadth of research on space debris in LEO, the research into space debris that solely considers the LEO space environment cannot be easily translated for MEO. For one, the environmental variables present in LEO significantly differ from those in other spectrums. Within LEO, atmospheric drag and solar radiation pressure can act upon debris and reduce the velocity of said debris and deorbit most within several years (Smith Et At, 2020). But MEO and higher orbital planes do not have these environmental mitigation factors, leaving debris in these spectrums to remain. As a result, research predicting the state of space debris within this environment assumes that the state of space debris in MEO is more severe. As stated by Tibault Maury, "Recent studies focusing on the flux of debris crossing the GEO region (Dongfang et al., 2017; Oltrogge et al., 2018), combined with recent anomalous events (NASA, 2018), suggest that the threat could be greater than it has been assumed until now. In a short term, the space debris pressure into the MEO region seems nonetheless less important (Johnson, 2010b)" (Maury, 2019). As such, when analyzing space debris within MEO, a different perspective is required.

However, in order to analyze the state of space debris within MEO, it will be beneficial to observe studies conducted in other areas to determine how space debris effects are evaluated. When looking at studies done with space debris in LEO, it has been shown that space debris does indeed have a measurable impact on the space environment. Space debris within the LEO spectrum has been shown to be increasing at an increasing rate due to the high level of activity taking place (Maury, 2019). As more satellites are placed within this spectrum in the coming years, it is projected that debris within this area will increase in a related fashion. And so by looking solely at this area, it is easy to assume that this conclusion can be extended to all other areas. However, this characterization cannot be fully validated for all spectrums due to the difference in variables present. And as such, the need for the study detailed in this paper arises.

MEO is much more susceptible to space debris than LEO. Due to the long-term nature of the environment, all actions have lasting effects that need to be accounted for. This does not mean to say that MEO cannot host space activity, just that proper management is required in order to protect the spectrum. As stated by Rossi et al., “accurate management of the MEO region, with de-orbiting of upper stages and re-orbiting of satellites at the end-of-life, can guarantee long term stability of the environment with very low collision risk, compatible with the delicate mission of the navigation constellations satellites. On the other hand, it should be stressed that similarly to the LEO region, the non-disposal of the upper stages significantly increases the long term growth of the collision risk in the region” (2009). The paper then goes on to say that deorbit attempts also do not harm other regions as the deorbiting debris passes through them, further encouraging disposal. Using this, it can be concluded that while the MEO region is a highly valuable area that needs to be protected, with proper mitigation and debris handling strategies, the MEO environment can be used sustainably.

Now that it has been established that the MEO environment is susceptible to space debris and mitigation strategies are required, it is important to learn the current state of space debris and its effect on the MEO space environment. While previous studies have been conducted that focus on the effects of space debris, most notably by Maury, this research does not consider the MEO environment. As such only predictions can be made about the MEO environment, and while conclusions such as the one offered assume that space debris will have an increased effect, there must be further analysis to prove if such claims are accurate. Therefore, this paper seeks to fill in the gap by evaluating to what extent Medium-Earth Orbital fragmentation events and resultant space debris has affected the corresponding space environment.

Hypothesis

The initial hypothesis for this research project was that the behavior of space debris in the space environment within Medium Earth Orbit would be similar to space debris behavior within Low-Earth Orbit, in that Medium-Earth Orbital fragmentation events and resultant space debris would have contributed to a steady measurable rise in spatial density. The justification for this hypothesis comes from studies done regarding space debris in Low-Earth Orbit and the resultant conclusions that stressed the rapid increase seen in space debris spatial density as a result of increased space activity over the years (Maury, 2019). Due to the similarities of the environments of LEO and MEO, it has been assumed that the behavior of space debris would remain similar despite the environmental differences of the two spectrums mentioned previously in the literature review. As such, the expected conclusion of this research is its conformity to previous research within the field.

Methodology

In order to evaluate the state of space debris in the Medium-Earth Orbit space environment, quantitative tracking data detailing the relevant characteristics of space debris within the defined spectrum must be analyzed. The required parameters include altitude (orbital height within defined region), attitude (orientation of selected debris), and relative velocity

(Δspeed of debris and simulated collision) (European Space Agency, 2020). These parameters allow for effective calculation, facilitating the drawing of accurate conclusions from the analysis that include the entire defined region. Within this paper, the quantitative data and the results from their analysis will allow for predictions of the effects of space debris on the MEO space environment over time.

With the use of tracking data and subsequent analysis, the methodology of this paper will follow that of a quantitative correlational statistic analysis. As mentioned earlier, the quantitative data regarding space debris in the derided spectrum will be used for analysis to evaluate the correlation between space debris and fragmentation events and the current state of the MEO space environment. The specifics of this research will be expanded on below.

The data for this study will be taken from the European Space Agency's Database and Information System Characterising Objects in Space (DISCOS). DISCOS is a publicly available database serving as a single-source reference for launch information, object registration details, launch vehicle descriptions, as well as spacecraft information (e.g. size, mass, shape, mission objectives, owner) for all trackable, unclassified objects which sum up to more than 40000 objects (European Space Agency, 2020). The data provided by DISCOS, once sufficiently evaluated for the current spectrum of analysis, will subsequently be analyzed by the European Space Agency's Meteoroid and Space Debris Terrestrial Environment Reference Version 8 (MASTER-8) tool for statistical analysis. The MASTER-8 tool was developed by the Institute of Space Systems at the Technische Universität of Braunschweig (IRAS/TUBS), Germany under contract of the European Space Agency (ESA) for the express purpose of "the characterisation of the natural and the man-made particulate environment of the Earth, and the fast and simple evaluation of the resulting effects on space missions"(European Space Agency, 2020), and allows for the evaluation of the space debris environment, as is the goal of this study, through the provided statistical analysis functions. Furthermore, the MASTER-8 toolkit consists of "flux and spatial density prediction tool(s) which combines a quick assessment of spatial density characteristics with high resolution flux results and additional analytical capabilities" (European Space Agency, 2020). The use of these tools will be expanded upon later in this section.

The DISCOS database was chosen due to its breadth of information regarding space debris and current satellites, allowing for accurate and up-to-date results that would be relevant to the current field. Any attempts at self-collection of data would be woefully inadequate for the analysis required to fulfill the purpose of the research so therefore the DISCOS database is used. Additionally, the DISCOS interface allows for better processing of information, improving analysis times and reducing hardware requirements. The MASTER-8 model was chosen due to its integration with the DISCOS database, improving data handling and reducing risk of errors in translation compared to if another tool was used. While there are such other tools within this userspace, most notably the NASA Orbital Debris Engineering Model Version 3.1 (ORDEM 3.1), the DISCOS database and MASTER-8 model were chosen due to their publically available nature and open source license, allowing for data acquisition and handling transparency for the benefits of research reproduction. When addressing concerns of differences in data, the "ESA's MASTER model was assessed against NASA's ORDEM 3.0 (Krisko et al., 2015). The study concludes that: (i) for non-GEO cases, both population match very well considering 1 m debris size; (ii) at 10 cm MASTER2009 fluxes are all somewhat higher than those of ORDEM 3.0, (iii) within the critical size range at the 1-cm edge, ORDEM 3.0 displays a flux matching that of MASTER-2009. In the important ISS region, ORDEM 3.0 shows a flux reduction of nearly an order of magnitude smaller than that of MASTER-2009" (Maury, 2019). Therefore, while there are some discrepancies within the two databases, they have both been validated as accurate for the spectrum being studied in this paper and as such the conclusions drawn from the data used are valid regardless of source.

Currently, for man-made debris, the MASTER-8 model has data for active satellites, spent payloads and upper stages, fragmentations from on-orbit explosions and collisions, launch and mission-related objects, surface degradation particles (paint flakes), Sodium Potassium (NaK) coolant droplets from Radar Ocean Reconnaissance Satellite (RORSAT) core ejection events, dust and slag from Solid Rocket Motor (SRM) firings, Multi-layer Insulation (MLI) from fragmentations, and ejecta (European Space Agency, 2020). Additionally, the MASTER-8 model also considers meteoroids as part of its debris calculation, with the meteorite simulation models of Divine-Staubach, Cour-Palais, Jenniskens/McBride, and GRÜN (European Space Agency, 2020).

All of these debris sources are considered within the chosen analysis period with a default reference epoch[2] of 11/01/2016 for the full 3 dimensional spectrum ranging from Low Earth Orbit (LEO) (6371 km) up to lunar altitude (500 000 km). For this entire range, DISCOS currently has data starting at the year 1960 to the year 2036. At the time of publication, the data ranging from the year 2020 to the year 2036 is predicted by the European Space Agency by an extrapolation of current trends. This data is seen as mostly accurate for the future, barring any extreme events.

Equipped with this data and analysis tools, in order to fulfill the purpose of this research, this paper will consider all provided debris sources, both man made and natural, within the defined spectrum of MEO (2000km - 35786km) and analyze the effects of space debris and fragmentation events on the MEO space environment. In regards to natural debris, the GRÜN

[2] Time Period of Analysis

model mentioned earlier will be used due to its recent implementation within the MASTER-8 model, allowing for a new evaluation of the space debris issue. For the purposes of this research, the Spatial Density function introduced earlier will be used to analyze the effects of space debris and fragmentation events on the Medium-Earth Orbit space environment. The spatial density function as provided by the MASTER-8 model allows for the calculation of space debris's 3-dimensional density within a certain reference area as defined by the user for one or multiple debris sources. The function uses the orbital parameters of lower and upper altitude, disinclination, and right ascension to set the limits for density analysis and create a 3 dimensional area in order to calculate the debris within that area at the specified time to find an average spatial density for the mentioned analysis epoch. While this process is significantly more in depth in regards to exact calculation and input parameters, a detailed explanation is out of the scope of this paper. For further explanation of the spatial density calculation process, consult Krisko Et Al. Returning to the study conducted, once the orbital parameters are defined for the spatial density function and the debris sources selected for analysis, the time period is defined by the user for final setting of the function parameters. Once this process is done and initialized, the toolkit will return the results of the spatial analysis for the defined region.

The research parameters of this study will be as follows. The study will consider all debris sources, both manmade and natural, as provided by the DISCOS database in calculations. All debris sources, as well as the GRÜN meteorite model, will be inputted into the relevant input data file (for reference below) for loading into the MASTER-8 toolsuite. The spatial density function will then be used with the orbital parameters of altitude [2000km; 35786km], declination [-90; 90°] with a 2° inclination interval, and ascension [-180; 180°] with a 10° interval in order to sample all possible orbital paths within Medium-Earth Orbit. In regards to altitude, a 100 km interval will be used to traverse the defined orbital range. The spatial density of debris within this range will then be computed for a time range of 1958 to 2036, with 2 year epochs, resulting in 39 resulting density calculations.

In order to conduct analysis, the MASTER-8 software toolsuite was installed on an X86_64 system running the OpenSuSE Tumbleweed operating system with the openJDK 1.8 package used for the Java runtime environment. To input the needed data files and expedite data handling, an automation program script written for the Bourne Again Shell (BASH) will be used in conjunction with the MASTER-8 toolsuite (Refer to Appendix A). The BASH file was placed in the MASTER-8 application directory along with the pre-configured input file (Refer to Appendix B). In regards to data, the condensed population files provided by the ESA were exported into the MASTER-8 data folder once verified and uncompressed. In order to ensure data integrity, all data files along with the MASTER-8 application file were verified with the corresponding MD5 checksum to ensure all data had not been tamped with. Following this, the BASH automation script was executed in the application directory. The script then edits the input file to insert the required parameters, then loads it within the MASTER-8 application for spatial density calculation. Once completed, the output files are saved for future reference. This action then repeats for all test cases until completion.

Results

Once all analysis periods had been completed, the results needed were parsed and cataloged for data entry and visualization. The results were exported into an Excel spreadsheet with the specified period and corresponding spatial density calculation as generated by the MASTER-8 function (see table below for results).

This table was then used to plot the average spatial density of debris in MEO in relation to time. The graph below (Figure 1) is the result of this visualization and represents all results from the conducted analysis. The vertical axis is the average spatial density in units of 1/m3 with the upper bound of 4.00E+07 and a lower bound of 0. On the horizontal axis of this plot is the epoch of the analogous spatial density figure in increments of two years. The figures used for the horizontal axis are the end year for the epoch analyzed, starting with 1960 and ending at the year 2036, as is the data limit for the condensed population files provided by the ESA. Additionally, error bars of ±10% have been included to accommodate any discrepancies in data as mentioned in the methodology section.

For a further breakdown of the results, Figures 2 through 9 have been provided. These plots are identical in data to Figure 1 but display the results in 8-year snapshots to better understand the micro-trends within the larger macro-trend of the data displayed. These plots will be referenced later in the following section.

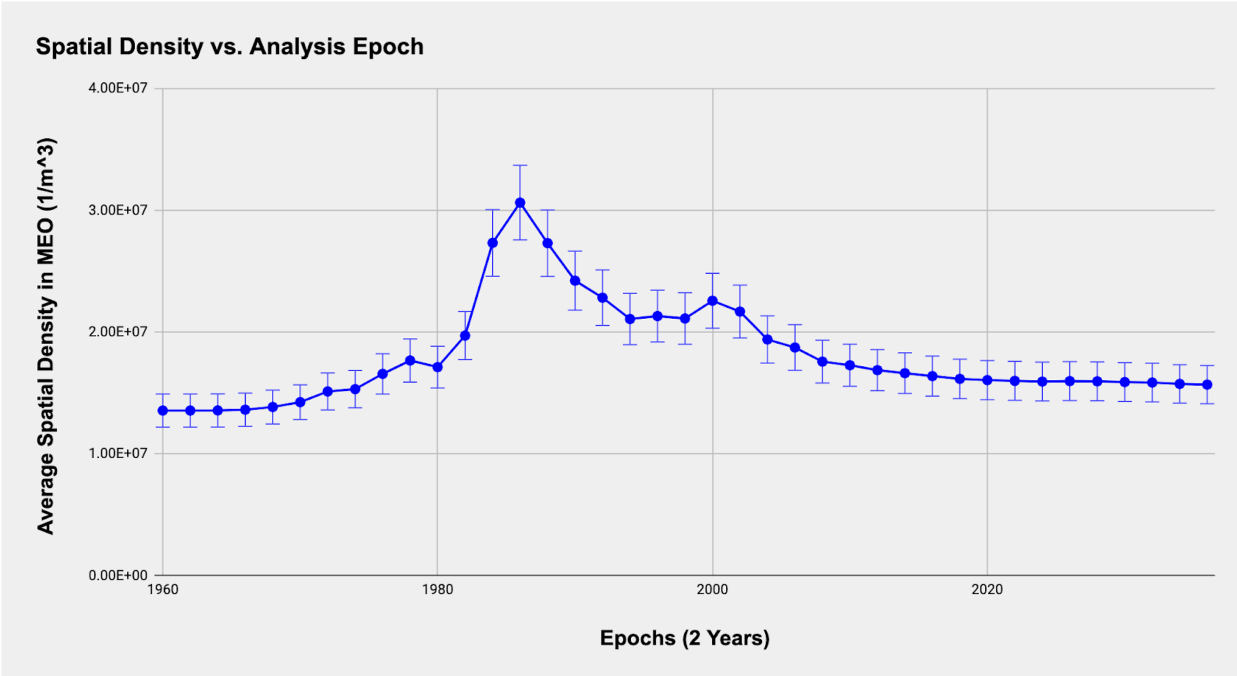

Figure 1: Average Spatial Density of Debris in MEO from 1960 to 2036

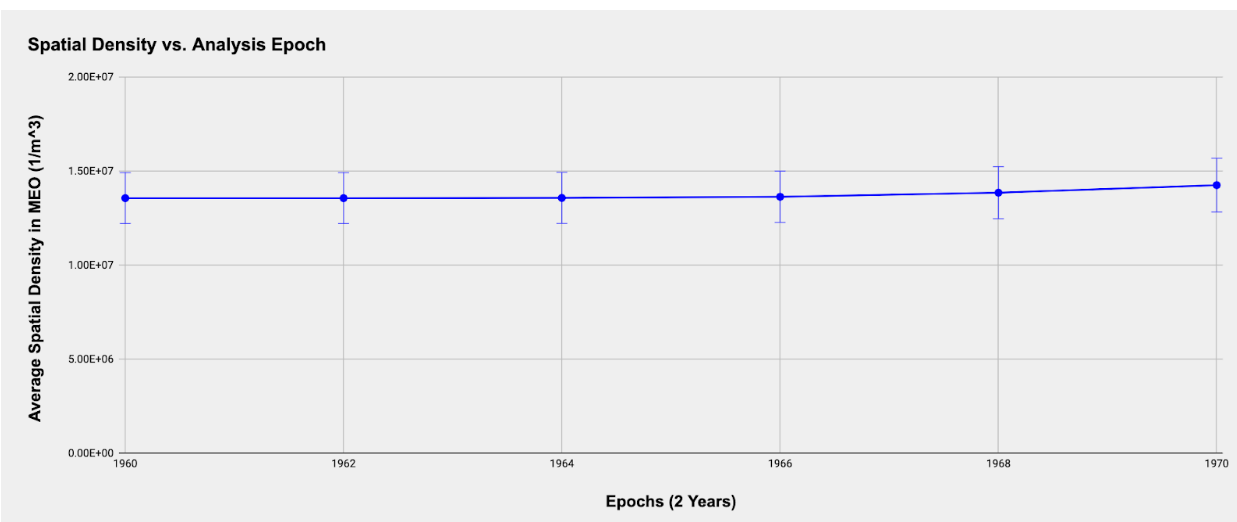

Figure 2: Average Spatial Density of Debris in MEO from 1960 to 1970

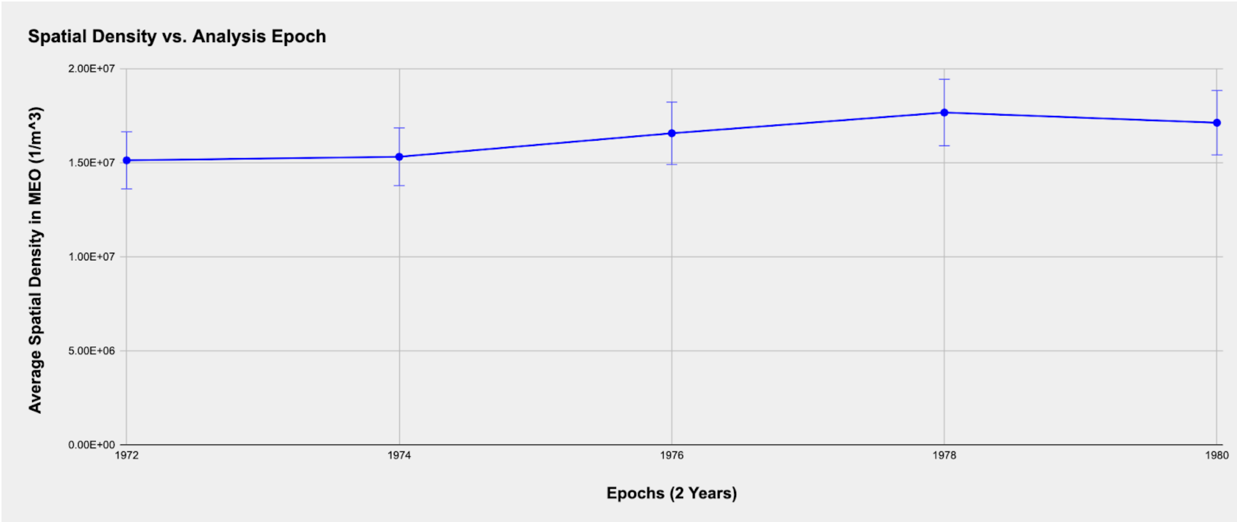

Figure 3: Average Spatial Density of Debris in MEO from 1972 to 1980

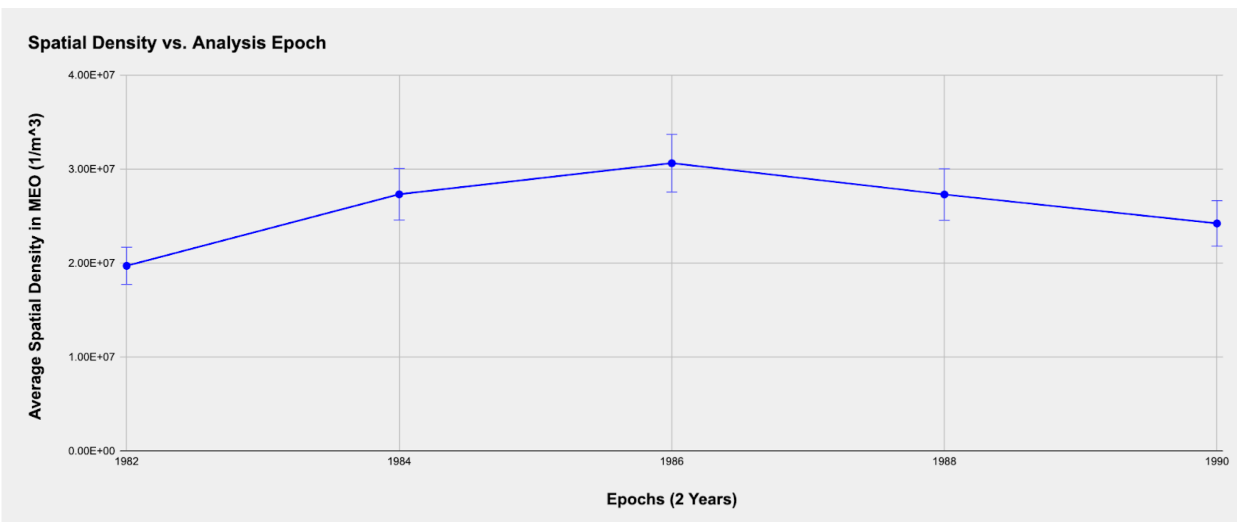

Figure 4: Average Spatial Density of Debris in MEO from 1982 to 1990

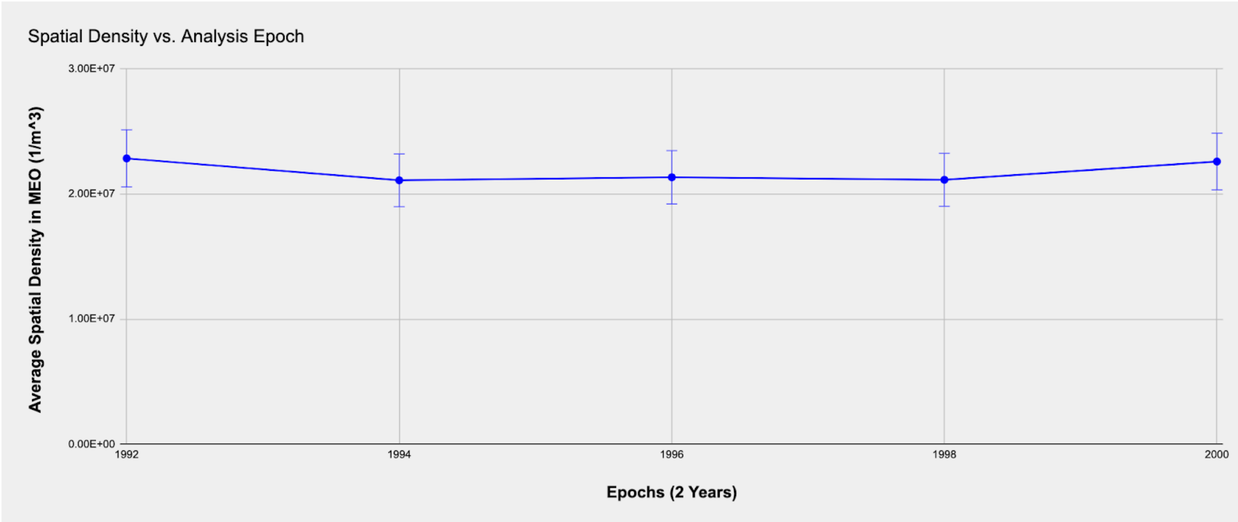

Figure 5: Average Spatial Density of Debris in MEO from 1992 to 2000

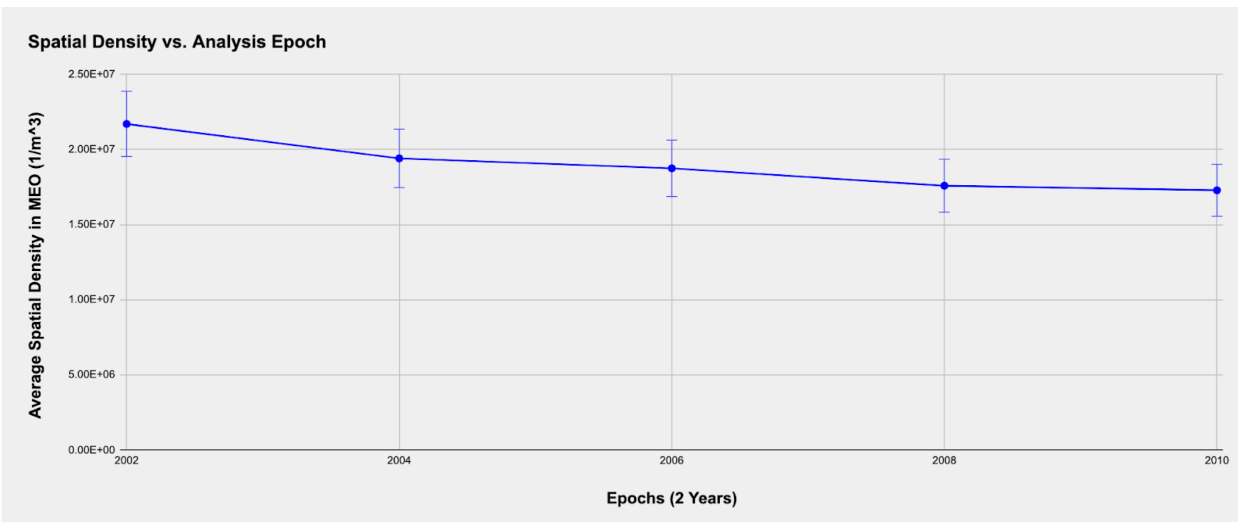

Figure 6: Average Spatial Density of Debris in MEO from 2002 to 2010

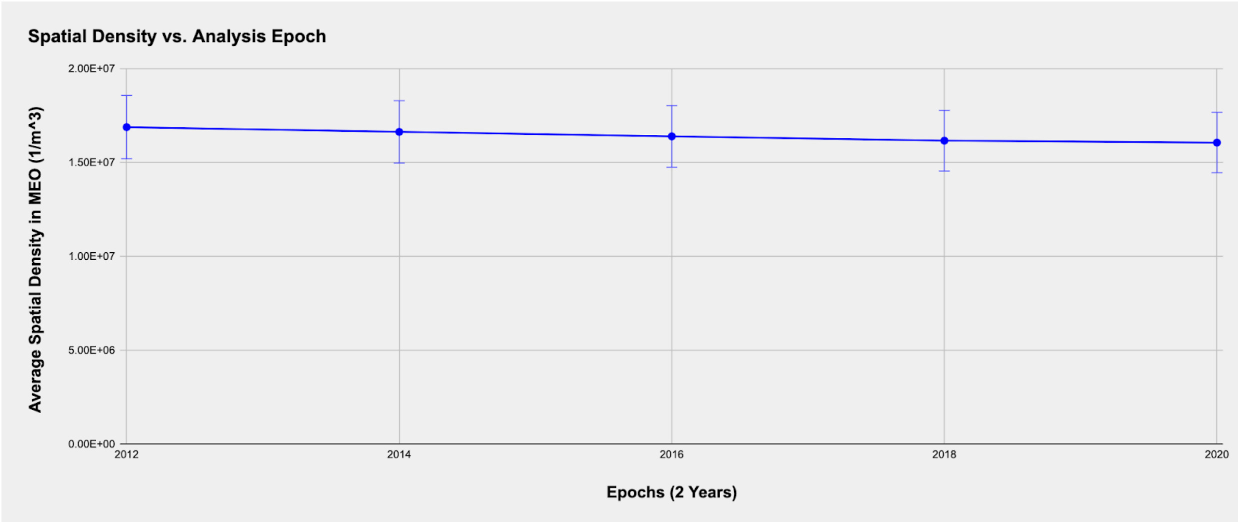

Figure 7: Average Spatial Density of Debris in MEO from 2012 to 2020

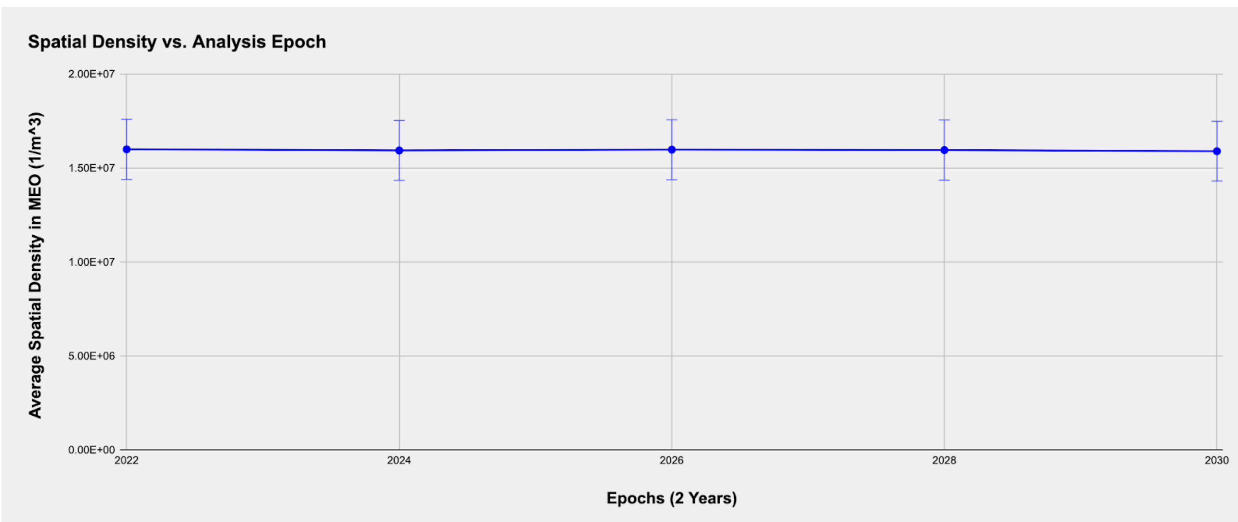

Figure 8: Average Spatial Density of Debris in MEO from 2022 to 2030

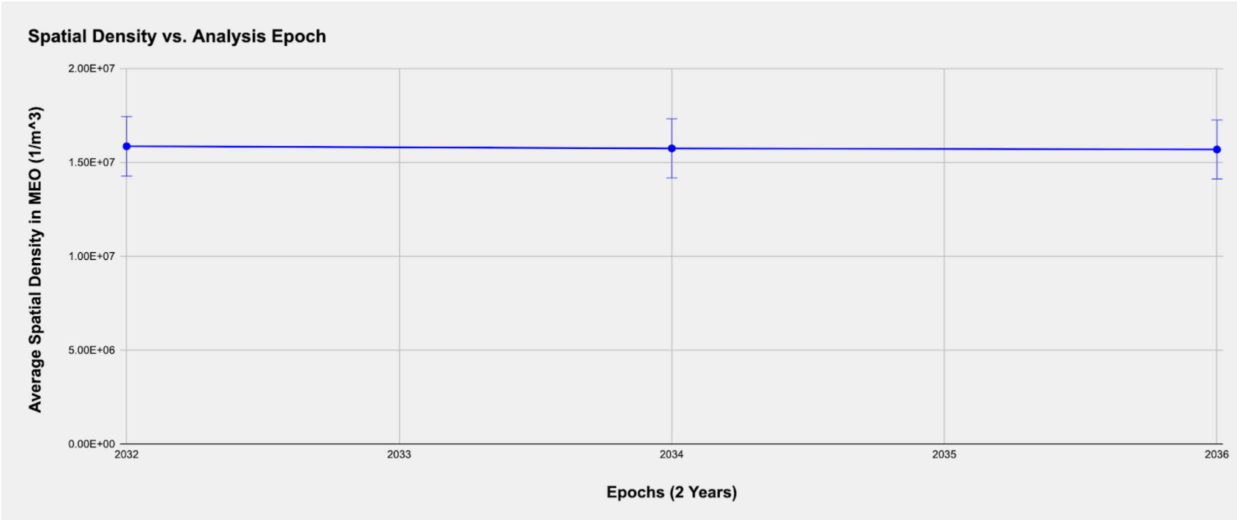

Figure 9: Average Spatial Density of Debris in MEO from 2032 to 2036

Analysis

The results displayed above show the general trend of space debris within the MEO spectrum. In order to facilitate an encompassing understanding of these results, the analysis portion has been divided into two actions: Trend Observation and Discussion of Trends. These sections will first define the data seen above and then offer possible causes for the environment analyzed.

Trend Observation

As displayed above, the average spatial density of debris within MEO is split into two time periods of relative stability, divided by a spike in activity from around 1980 to 2000. For the first period of stability, average spatial density of debris remained around 1.40E+07/m^3 . This continued from 1960 to the mid 1970s. After this, it can be seen that a slight uptick in activity occurs until 1980 where the initial spatial density increases from 1.40E+07/m^3 to 1.75E+07/m^3. From 1980 to 1986, the average spatial density increased by 118% from 1.75E+07/m^3 to the all time peak of 2.07E+07/m^3. From this time onwards, the average spatial density retains a general downward trend, stagnating near the late 1990s but continuing downward from there. Overall, the start and end states of the average spatial density within the MEO spectrum are 1.36E+07/m^3 and 1.57E+07/m^3 respectively, only differing by 0.21/m^3. For the subsequent plots, the data remain the same, however, the time period is displayed in snapshot time periods of 10 years to display trends for each decade. Within these plots, it is seen that disregarding the plots from before 2002, measured spatial density of debris is trending slightly downwards or remaining at the same level, indicating a relatively stable environment.

Discussion of Trends

As evidenced by the graphs displayed above, the trends seen in the average spatial density of space debris do not conform to the initial hypothesis stated earlier. While it was assumed that the trends of the spatial density of debris within LEO, where said density was increasing at an increasing rate, would be applicable to the trends of debris within MEO, this seems to not be the case. As stated above, the density of space debris remains stable within the defined spectrum, subverting expectations that debris would continue to rise as activity within MEO continues to escalate (Maury, 2019). While there was a spike from around 1980 to 2000, debris levels have remained stable since with post-spike levels almost down to pre-spike levels. When looking at the 10-year snapshots, this becomes even more evident, further supporting this conclusion. As such, it would be inaccurate to characterize the MEO space environment as similar to the LEO space environment. As a result of this data analysis and characterization, it can be answered with relative confidence that the Medium-Earth Orbital fragmentation events and resultant space debris has not affected the Medium-Earth orbit space environment to a significant extent due to the stable levels of debris present within this spectrum.

Conclusion

Moving on to limitations, there are some aspects of this research that can be improved upon in future iterations. Most limitations of this study stem from a limit in computational resources and limited analysis parameters. While the research conducted is fundamentally sound, in future iterations, the analysis conducted would benefit from more advanced computational studies as due to hardware limitations at the time of analysis, parameters for data simulation had to be broader. The interval traversed for analysis, the time epoch limits, altitude ranges, and other simulation parameters would benefit from higher specification hardware. Additionally, better data traversal tools would have allowed for analysis of the cell passage events and standard environment interface data files used for the spatial density calculation; this again was limited by the computational resources at the time. And so, while this study was able to effectively characterize the space environment, better tools would have allowed for more micro-analysis.

In regards to the implications of this study, this research has the potential to inform further analysis of the MEO space environment, with further research being able to conduct a full risk-assessment as has been similarly done for the LEO environment (Aida & Kirschner, 2011). Additionally, the findings of this study raise questions regarding the mitigation of space debris and how the MEO environment differs from the LEO environment. Using what has been learned in this study, further analysis can be conducted regarding the difference between the two environments and the positive trends that are seen in each area.

Overall, this study exploring the effects of space debris and fragmentation events on the Medium-Earth Orbit space environment was able to effectively analyze the state of the defined area and address the goals of the research project. It was able to fill in a gap in the existing body of research that future inquiries will be able to build upon. While there were limitations in analysis within the study due to the availability of resources at the time of inquiry, the study was able to characterize the space environment and provide analysis to an acceptable degree. As humans continue to venture out into space, this research will hopefully be relevant in allowing for future exploration throughout our space environment.

Appendix A

```
#! /bin/bash

#notes
#Place Script in Master Directory


for (( startYear = 1958 ; startYear <= 2034 ; startYear += 2 ));
do

    #declares end year for simulation
    endYear=$(($startYear+2))
    dataDirectory=[$startYear]-[$endYear]_MASTER-8_Data

    #makes directories to store data
    mkdir $dataDirectory
    mkdir $dataDirectory/output
    mkdir $dataDirectory/input


    #copies acsii files to directory

    cp masterFiles/input/master.inp $dataDirectory/input
    cp masterFiles/input/default.con $dataDirectory/input
    cp masterFiles/input/default.def $dataDirectory/input
    cp masterFiles/input/default.sdf $dataDirectory/input
    cp -R masterFiles/input/focus $dataDirectory/input



    #replacing paths on master.cfg
    sed -i "24s|.*|  $dataDirectory/output/ -(120 char)-       Output path|"
master.cfg
    sed -i "27s|.*|  $dataDirectory/input/ -(120 char)-       Input path|"
master.cfg
    sed -i "28s|.*|  $dataDirectory/input/focus -(120 char)-       Input path|"
master.cfg

    #no need to change data directory stuff

    cd $dataDirectory

    #replacing years on master.inp
    sed -i "27s|.*|$dataDirectory-Run|" input/master.inp
    sed -i "34s|.*| $startYear 01 01 00 -(yyyy mm dd hh)- Begin|" input/master.inp
```

```
    sed -i "35s|.*| $endYear 12 31 23 -(yyyy mm dd hh)- End|" input/master.inp

    #exit directory
    cd /home/linux/MASTER-8.0.2


    #copy config file for refrence
    cp master.cfg $dataDirectory/input

    #run simulation
    ./master-linux64

    #copies logfiles
    cp progress.dat $dataDirectory/
    cp logfile $dataDirectory/

done
exit 0
```

Appendix B

```
#----<ESA-MASTER>--------------------------------------------------------------
#
#          __/_/  __/__/  __/__/   _/__/_/ __/__/__/ __/__/__/ __/_/__/
#         __/ _/__/ __/ __/   __/ __/        __/    __/       __/    __/
#        __/  __/  __/ __/__/__/  __/__/    __/    __/__/    __/_/__/
#       __/       __/ __/   __/      __/   __/    __/       __/    __/
#      __/       __/ __/   __/ _/__/_/    __/    __/__/__/ __/     __/
#
# __ ESA Meteoroid & Space Debris Terrestrial Environment Reference Model__
#-----------------------------------------------------------------------------
# Purpose: Definition of execution parameters of the MASTER command line tool.
#-----------------------------------------------------------------------------
# Note: Lines which may be edited by the user are NOT marked by comment
#       sign ('#').
#-----------------------------------------------------------------------------
#
#-----------------------------< Run Settings >--------------------------------
# Note: Give the program run a name and a comment. Do NOT modify or
#       remove the '-(27 ' sequence since it serves as End of String marker.
#-----------------------------------:-----------------------------------------
# Run identifier (used as output file prefix)
#-------------------------|
master                      -(27 char)-
#
# Run comment (2 lines, appears as header in any output file and in plots)
#----------------------------------------------------------------------|
[1958]-[1960]_MASTER-8_Data-Run

#
#----------------------------< Time Settings >--------------------------------
# Note: Specify start and end of the analysis epoch.
#-----------------------------------:-----------------------------------------
# Begin and end of analysis time interval
 1958 01 01 00 -(yyyy mm dd hh)- Begin
 1960 12 31 23 -(yyyy mm dd hh)- End
#
#--------------------------< Impactor Settings >------------------------------
# Note: Specify which source terms and size/mass ranges shall be considered
#       for the analysis.
#-----------------------------------:-----------------------------------------
# Source switches (0=off,1=on)
  0             -(0,1)-            Explosion Fragments
  0             -(0,1)-            Collision Fragments
  0             -(0,1)-            Launch/Mission related objects
```

```
  0               -(0,1)-           NaK-droplets
  0               -(0,1)-           SRM slag
  0               -(0,1)-           SRM Al2O3 dust
  0               -(0,1)-           Paint flakes
  0               -(0,1)-           Ejecta
  0               -(0,1)-           MLI
  1               -(0,1)-           Man-made population (all individual sources
above will be disabled)
  1               -(0,1)-           Meteoroids
  0               -(0,1)-           Clouds
#
# Cloud file identifier

#
# Constellation projection switch (0=off,1=on)
  1               -(0,1)-           0 = no constellation projection for TLE
#                                   1 = use const. projection for TLE Backgr.
#
# Annual meteoroid stream consideration switch
  0               -(0:2)-           0 = no seasonal met. streams (averaging)
#                                   1 = seasonal met. streams (Jenniskens)
#                                   2 = seasonal met. streams (Cour-Palais)
#
# Background meteoroid model consideration swith
  2               -(0:2)-           0 = no background meteoroids
#                                   1 = background meteoroids (Divine-Staubach)
#                                   2 = background meteoroids (Gruen)
#
# Background meteoroid population switches (0=off,1=on)
  1               -(0,1)-           Core population
  1               -(0,1)-           Asteroidal population
  1               -(0,1)-           A population
  1               -(0,1)-           B population
  1               -(0,1)-           C population
#
# Velocity distribution for GRÜN meteoroid model
  0               -(0:1)-           0 = Grün (constant velocity 20 km/s)
#                                    1 = Taylor distribution
#
# Analysis size/mass thresholds
  1.00000e-06 m   -(value (m,kg))-   Lower threshold
  1.00000e+02 m   -(value (m,kg))-   Upper threshold
#
#---------------------------< Target Settings >------------------------------
# Note: Specify the type of target to be analyzed.
#-----------------------------------:---------------------------------------
# Analysis mode
```

```
  3               -(1:4)-           1 = orbiting target
#                                   2 = inertial volume
#                                   3 = spatial density
#                                   4 = lagrange point  (non-Earth-bound)
#
# Target type
  1               -(1:3)-           1 = sphere
#                                   2 = randomly tumbling plate
#                                   3 = oriented surface (defined in .sdf file)
#
# Target properties (only if analysis mode 1 and propagation requested)
# Value___________Unit______________Description______________________________
   9710.0                    -(kg)-           Mass                   (default:
1000.0)
   39.130                    -(m**2)-           Cross section (drag) (default:
10.0)
   39.130                    -(m**2)-           Cross section (SRP) (default:
10.0)
   2.2000                    -( - )-           Drag coefficient (default: 2.2)
   0.0000                    -( /d )-           Drag coefficient rate (default:
0.0)
   1.3000                    -( - )-           Reflection coefficient (default:
1.3)
#

# Target orbit propagation resolution (only in analysis mode 1)
  4               -(1:4)-           1 = 1 month
#                                   2 = 3 months
#                                   3 = 6 months
#                                   4 = 1 year
#
# Target orbit(s) (considered only in analysis mode 1)
# Prop.sw   start epoch      end epoch    SMA        ECC        INC     RAAN
AoP
#___0/1____yyyy_mm_dd_hh__yyyy_mm_dd_hh___[km]_______[-]______[deg]____[deg]____[de
g]___
     0     2016 11 01 00  2016 11 01 00  7164.30  1.000e-03  98.2400  0.568100
93.9282
#...
#
# Orbital arc (considered only in analysis mode 1)
   0.0000         -(deg)-           Lower argument of true latitude
   360.00         -(deg)-           Upper argument of true latitude
#
# Inertial volume position (considered only in analysis mode 2)
   7178.0         -(km)-            Geocentric distance
   0.0000         -(deg)-           Right ascension
```

```
   0.0000         -(deg)-            Declination
#
# Spatial density profile range (considered only in analysis mode 3)
   2000.0         -(km)-             Lower altitude limit
   36786          -(km)-             Upper altitude limit
  -90.000         -(deg)-            Lower declination limit
   90.000         -(deg)-            Upper declination limit
  -180.00         -(deg)-            Lower right ascension limit
   180.00         -(deg)-            Upper right ascension limit
#
#---------------------< Definition of Input File Names >----------------------
# Note: Give the name of additional input files to be used (do NOT modify or
#       remove the '-(120 ' sequence since it serves as End of String marker).
#----------------------------------:-----------------------------------------
  default.def     -(120 char)-       Basic output spectrum definition file
  default.sdf     -(120 char)-       Surface description file
  default.con     -(120 char)-       Constellation descript. file
#
#-----------------------< Basic Output Settings >---------------------------
# Note: Activate or de-activate spectrum and data output.
#----------------------------------:-----------------------------------------
# Differential spectra
  1               -(0,1)-            0 = don't generate differential spectra
#                                    1 = generate differential spectrum files
# Cumulative spectra
  1               -(0,1)-             0 = don't generate cumulative spectra
#                                    1 = generate cumulative spectrum files
# Reverse cumulative spectra
  1               -(0,1)-            0 = don't generate reverse cumulative spec.
#                                    1 = generate reverse cumulative spec. file
# Additional dump of CPE data (experts feature)
  0               -(0,1)-            0 = don't dump cell passage characteristics
#                                    1 = dump CPE        (ATTENTION: spacious!)
# Additional dump of STENVI data (experts feature)
  0               -(0,1)-            0 = don't dump STENVI
#                                    1 = dump STENVI     (ATTENTION: spacious!)
#
# STENVI definition of output spectrum
# Bin       Min          Max
    36 -1.80000e+02  1.80000e+02     Azimuth   [deg]
    10 -9.00000e+01  9.00000e+01     Elevation [deg]
    20  0.00000e+00  2.00000e+01     Velocity  [km/s]
     6  1.00000e-06  1.00000e+01     Diameter  [m]
     1  0.00000e+00  3.60000e+02     Argument of true Latitude [deg]
     5  0.00000e+00  5.00000e+00     Density   [g/cm^3]
#
# Switch for indication of uncertainty bars (2D-plot)
```

```
  1               -(0,1)-            0 = don't plot uncertainty bars
#                                    1 = plot uncertainty bars
#
#--------------------------< Damage Law Settings >---------------------------
# Note: Set calibration parameters for the conchoidal diameter damage equation
#       if you plan to analyze flux vs. impact feature size on britte surfaces
#       (see user manual for details).
#----------------------------------:-----------------------------------------
# Calibration parameters for conchoidal diameter damage equation
   1.0000         -(--)-             Dh/dp ratio
   1.0000         -(--)-             Correction factor to the Taylor formula
   0.0000         -(mu)-             Taylor diameter reduction
   0.0000         -(mu)-             Minimum Taylor diameter Dmin
   12000          -(mu)-             Conchoidal interception diameter
   100.00         -(mu)-             Mean diameter for Gauss filter
   4.0000         -(--)-             Standard deviation for Gauss filter
   0.80000        -(--)-             Gauss factor
#
#
#
#
#
#--eof-------------------------------------------------------------------eof---
```

References

Aida, S., & Kirschner, M. (2011). Collision risk assessment and operational experiences for LEO satellites at GSOC.

Colombo, C., & Gkolias, I. (2017). Analysis of orbit stability in the geosynchronous region for end-of-life disposal. In *7th European Conference on Space Debris, ESA/ESOC* (pp. 1-14). ESA.

Del Portillo, I., Cameron, B. G., & Crawley, E. F. (2019). A technical comparison of three low earth orbit satellite constellation systems to provide global broadband. *Acta Astronautica*, *159*, 123-135.

European Space Agency. (2020). MASTER-8: Software User Manual. Retrieved from https://sdup.esoc.esa.int/master/downloads/documentation/8.0.2/MASTER-Software-User-Manual.pdf

Jenkin, A. B., & McVey, J. P. (2009, March). Constellation and "Graveyard" Collision Risk for Several MEO Disposal Strategies. In *Proceedings of the Fifth European Conference on Space Debris, ESA SP-672, CD-ROM, ESA Communication Production Office, Noordwijk, The Netherlands*.

Johnson, N. L. (2010). Medium Earth Orbits: is there a need for a third protected region?.

Krisko, P. H., Flegel, S., Matney, M. J., Jarkey, D. R., & Braun, V. (2015). ORDEM 3.0 and MASTER-2009 modeled debris population comparison. *Acta Astronautica*, *113*, 204-211.

Liou, J., & Johnson, N. L. (2006). Risks in space from orbiting debris. *SCIENCE-NEW YORK THEN WASHINGTON-*, *311*(5759), 340.

Maury, T. (2019). *Consideration of space debris in the life cycle assessment framework* (Doctoral dissertation, Bordeaux).

Mehrholz, D., Leushacke, L., Flury, W., Jehn, R., Klinkrad, H., & Landgraf, M. (2002). Detecting, tracking and imaging space debris. *ESA Bulletin(0376-4265)*, (109), 128-134.

Rossi, A., Anselmo, L., Pardini, C., & Jehn, R. (2009, March). Effectiveness of the de-orbiting practices in the MEO region. In *Proceedings of the Fifth European Conference on Space Debris, ESA SP-672, CD-ROM, ESA Communication Production Office, Noordwijk, The Netherlands*.

Smith, B. G. A., Capon, C. J., Brown, M., & Boyce, R. R. (2020). Ionospheric drag for accelerated deorbit from upper low earth orbit. *Acta Astronautica*, *176*, 520-530.

Works Consulted

Akahoshi, Y., Nakamura, T., Fukushige, S., Furusawa, N., Kusunoki, S., Machida, Y., ... & Cho, M. (2008). Influence of space debris impact on solar array under power generation. *International Journal of Impact Engineering*, *35*(12), 1678-1682.

Grassi, L., Tiboldo, F., Destefanis, R., Donath, T., Winterboer, A., Evans, L., ... & Gelhaus, J. (2014). Satellite vulnerability to space debris–an improved 3D risk assessment methodology. *Acta Astronautica*, *99*, 283-291.

Gulde, M., Kempf, S., & Schäfer, F. (2016). Fast and Flexible Space Debris Risk Assessment for Satellites. *Journal of Space Safety Engineering*, *3*(3), 111-113.

Hirai, T., Higashide, M., Kurosaki, H., Kawakita, S., Hasegawa, S., Mando, Y., ... & Tanaka, K. (2017). Re-examination of electrical failure risk on satellite's power harnesses caused by space debris impacts: simultaneous measurements of sustained discharge and plasma density. *Procedia engineering*, *204*, 445-451.

Horstmann, A., Krag, H., & Stoll, E. (2019). Providing Flux Uncertainties in ESA-MASTER: The Accuracy of the 1cm Population. *LPI Contributions*, *2109*, 6015.

Nikolaev, S., Phillion, D., Springer, H. K., deVries, W., Jiang, M., Pertica, A., ... & Olivier, S. (2012). *Brute Force Modeling of the Kessler Syndrome* (No. LLNL-CONF-579617). Lawrence Livermore National Lab.(LLNL), Livermore, CA (United States).

Vananti, A., Schildknecht, T., & Krag, H. (2017). Reflectance spectroscopy characterization of space debris. *Advances in space research*, *59*(10), 2488-2500.

Walker, R., Klinkrad, H., Sdunnus, H., & Stokes, H. (2001). Update of the ESA space debris mitigation handbook. *EUROPEAN SPACE AGENCY-PUBLICATIONS-ESA SP*, *473*, 821-826.

Welty, N., Rudolph, M., Schäfer, F., Apeldoorn, J., & Janovsky, R. (2013). Computational methodology to predict satellite system-level effects from impacts of untrackable space debris. *Acta Astronautica*, *88*, 35-43.